Isothermal Crystallization and Melting Behavior of Polypropylene with Lanthanum Complex of Cyclodextrin Derivative as a β-Nucleating Agent

Anran Zeng,[1] Yuying Zheng,[2] Shangchang Qiu,[1] Yong Guo[1]

[1]*College of Chemistry and Chemical Engineering, Fuzhou University, Fuzhou 350108, China*
[2]*College of Materials Science and Engineering, Fuzhou University, Fuzhou 350108, China*

Received 12 November 2010; accepted 15 January 2011
DOI 10.1002/app.34183
Published online 12 April 2011 in Wiley Online Library (wileyonlinelibrary.com).

ABSTRACT: A novel highly active β-nucleating agent, β-cyclodextrin complex with lanthanum (β-CD-MAH-La), was introduced to isotactic polypropylene (iPP). Its influence on isothermal crystallization and melting behavior of iPP was investigated by differential scanning calorimeter (DSC), wide-angle X-ray diffraction (WAXD), and polarized light microscopy (PLM). WAXD results demonstrated that β-CD-MAH-La was an effective β-nucleating agent, with β-crystal content of iPP being strongly influenced by the content of β-CD-MAH-La and the isothermal crystallization temperature. The isothermal crystallization kinetics of pure iPP and iPP/β-CD-MAH-La was described appropriately by Avrami equation, and results revealed that β-CD-MAH-La promoted heterogeneous nucleation and accelerated the crystallization of iPP. In addition, the equilibrium melting temperature (T_m^0) of samples was determined using linear and nonlinear Hoffman-Weeks procedure. Finally, the Lauritzen-Hoffman secondary nucleation theory was applied to calculate the nucleation parameter (K_g) and the fold surface energy (σ_e), the value of which verify that the addition of β-CD-MAH-La reduced the creation of new surface for β-crystal and then led to faster crystallization rate. © 2011 Wiley Periodicals, Inc. J Appl Polym Sci 121: 3651–3661, 2011

Key words: polypropylene; isothermal crystallization; melt; **β**-nucleating agent; complex of cyclodextrin derivative

INTRODUCTION

Isotactic polypropylene (iPP) is a thermoplastic polymer which has been found in a wide range of applications in many fields because of their good mechanical properties and easy processability at a relatively low cost. As a typical semicrystalline polymer, iPP is a polymorphic material with several crystal modifications including α, β, and γ forms.[1] The intrinsic architecture and extrinsic parameters have a significant effect on crystallization behavior and morphological features, which are probably the most important factors affecting the final physical properties.[2] Therefore, the control of the growth rate and tailoring the proportion of different polymorphs is crucial for iPP applications. β-form isotactic polypropylene (β-iPP) attracts great attention due to its better properties, especially the better impact toughness and drawability in comparison with the more common α-form.[3,4] However, a higher proportion of β-iPP can be obtained only through special crystallization procedures, where the addition of nucleating agent is the most effective and accessible method.[1,5–7] These nucleating agents have been derived into four categories. The first category is organic pigment, such as γ-quinacridone (Dye Permanent Red E3B)[8] and triphenodithiazine[9]; the second one includes a minority of aromatic amide compounds, such as *N*,*N*′-dicyclohexil-naphthalene-dicarboxamide (NJ-Star)[10] and *N*,*N*′-dicyclohexyl-terephthalamide (TMB5)[11]; the third one contains some metal salts and their mixtures with some specific ligands, such as the two component system of $CaCO_3$ and pimelic acid,[12,13] Ca-salt of pimelic and suberic acids,[14] complexes of lanthanum and calcium (WBG)[2] and nano-$CaCO_3$ supported β-nucleating agent[15]; the four category includes some amorphous polymeric nucleating agents, such as styrene acrylonitrile (SAN) and polystyrene (PS).[16,17] However, to the best of our knowledge, no reports were concerned about that lanthanum complex with specific ligand of cyclodextrins (CDs) which are cone-shaped with a hydrophobic cavity and hydrophilic surface could act as β-nucleating agent for isotactic polypropylene.

Correspondence to: Y. Zheng (yyzheng_217@yahoo.cn, yyzheng@fzu.edu.cn).

Contract grant sponsor: Important Item of Science and Technology of Fujian Province; contract grant number: 2007HZ0001-2.

Contract grant sponsor: Scientific and Technological Personnel Service Enterprise Item of Ministry Science and Technology of China; contract grant number: 2009GJC40029.

Generally, the mechanical and physical properties of crystalline polymer depend on their crystalline structure and greatly affected by the crystallization process.[18–20] Therefore, the study of crystallization kinetics with β-nucleating agent is necessary for optimizing industrial condition for forming β-iPP. The isothermal and nonisothermal crystallization kinetics of iPP with different kinds of β-nucleating agents had been investigated by several studies.[2,21–26] Xiao et al.[2] investigated the isothermal crystallization kinetics of virgin iPP and two β-nucleated iPP systems based on rare earth complex (WBG) and *N*,*N*′-dicyclohexyl-terephthalamide (TMB5). The Kinetic parameters obtained from Avrami equation indicated that both agents increased the crystallization rate and shortened the crystallization time of iPP significantly. Bai et al.[24] comparatively studied isothermal crystallization behavior of iPP nucleated with individual α- and β-nucleating agent and compounding two nucleating agents. They also analyzed in detail the isothermal crystallization kinetics and crystallization structure. Zhao et al.[25] found IIB salts of alicyclic dicarboxylate acid was an effectively β-nucleating agent for iPP and investigated its effects on the crystallization kinetics of iPP using the Caze method. The results showed that the crystal growth pattern of nucleated iPP was heterogeneous nucleation. Zhang et al.[26] investigated the nonisothermal crystallization kinetic of iPP nucleated with a novel highly efficient supported β-nucleating agent (NA100), calcium pimelate (CaHA) supported on the surface of nano-$CaCO_3$. These results showed that Avrami and Mo's equation can be used to describe the nonisothermal crystallization kinetic of β-nucleated iPP.

Isothermal crystallization kinetics of polymer has been commonly studied by Avrami equation[27,28] and Hoffman-Lauritzen theory.[29] The former describes an overall crystallization rate, and the latter suggests the crystallization is controlled by nucleation and transport of the macromolecules in the melt. The objective of this article was to analyze the influence of β-cyclodextrin complex with lanthanum on the structure and isothermal crystallization behaviors of iPP. The melting behaviors following the isothermal crystallization process were also discussed. Moreover, the equilibrium melting temperature was determined using linear and nonlinear Hoffman-Weeks procedure. The spherulitic growth rate was used to obtain data on the specific surface free energies for the α- and β-crystal.

EXPERIMENTAL

Materials

Isotactic polypropylene (iPP, T30s) with a melt flow rate (MFR) of 3.881 g/10 min (230°C, 2.16 kg) was purchased from Fujian Petrochemical, Quanzhou, China.

The β-nucleating agent is a lanthanum complex of maleic anhydride β-cyclodextrin derivative (β-CD-MAH-La), which is synthesized as follows. First, modified β-CD carrying four vinyl carboxylic acid groups (β-CD-MAH) was prepared by dissolving β-CD (0.01 mol) and MAH (0.1 mol) into DMF. After continuously stirring at 75°C for 8 h, the mixture was cooled to room temperature. Trichloromethane was added and white precipitate was yielded, which is β-CD-MAH. Second, β-CD-MAH-La was synthesized by adding lanthanum chloride (0.12 mol) to the aqueous solution of β-CD-MAH (0.01 mol) and triethylamine was used as absorb acid agent. After continuously stirring for 10 h, the pale yellow power was obtained, which was β-CD-MAH-La.

β-CD-MAH-La was characterized by Fourier Transform infrared spectroscopy (FTIR), Element Analysis (EA). The inferred molecular structure of β-CD-MAH-La is $C_{42}H_{66}O_{31}(OCOCH{=}CHCOO)_{4}\text{-}La_9Cl_{23}]_n$. And according to TG results under nitrogen atmosphere, β-CD-MAH-La has excellent thermal stability.

Sample preparation

The iPP pellets and the nucleating agent β-CD-MAH-La were mixed by high-speed mixer for 5 min. Then the mixture was extruded by a twin-screw extruder (SJSH-30) through a strand die and pelletized. During the extrusion, the screw speed was set as 100 r/min and the temperature was 190–210°C from the hopper to die.

Characterization

Wide angle X-ray diffraction (WAXD)

The structure of pure iPP and iPP/β-CD-MAH-La under isothermal crystallization condition was examined by WAXD. For sample preparation, iPP pellets were placed between two glass slides on a hot stage kept at 220°C and kept for 10 min at this temperature to erase any thermal history, and melt-pressed to form a film, and then rapidly cooled to the crystallization temperature (T_c) and kept at this temperature for 2 h to allow crystallization at T_c. The final sample was then rapidly cooled to room temperature for test. WAXD experiments were conducted with a Rigaku MiniFlexII X-ray diffractionmeter (Cu Kα, λ = 1.54 Å). The spectra were recorded in the 2θ range between 10° and 30°, at the scanning rate of 2°/min. In the current work, analysis of the WAXD patterns were done using peak fitting with Gaussian and Lorentzian function after background subtraction.[16,22]

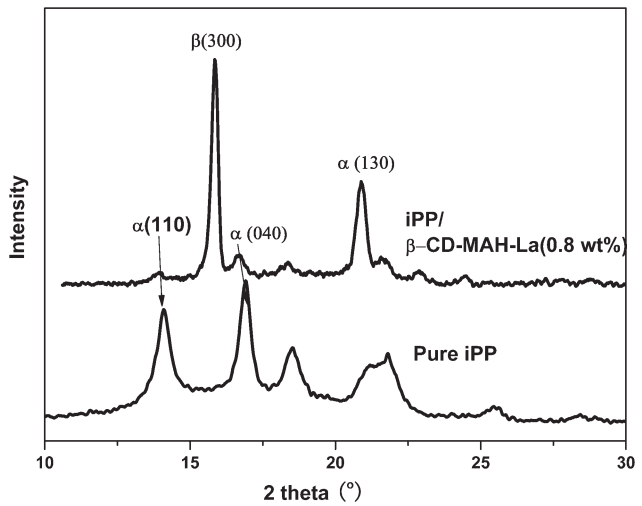

Figure 1 WAXD patterns of pure iPP and 0.8 wt % β-CD-MAH-La nucleated iPP crystallized at 130°C under quiescent condition for 2 h.

The relative content of β-crystal was calculated according to Turner Jones equation[16,30]:

$$K_\beta = \frac{A_{\beta(300)}}{A_{\alpha(110)} + A_{\alpha(040)} + A_{\alpha(130)} + A_{\beta(300)}} \quad (1)$$

$$X_{\text{all}} = 1 - \frac{A_{\text{amorphous}}}{\Sigma A_{\text{crystallization}} + A_{\text{amorphous}}} \quad (2)$$

where K_β denotes the relative content of β-crystal with respect to α-crystal. $A_{\alpha(110)}$, $A_{\alpha(040)}$, and $A_{\alpha(130)}$ represent the areas of α(110), α(040), α(130) planes at diffraction angles $2\theta = 14.1°$, 16.9°, 18.8°, respectively, while $A_{\beta(300)}$ represents the area of the β(300) plane at $2\theta = 16°$. $A_{\text{amorphous}}$ is the area of the amorphous peak.

The crystallite's size, D_{hkl} of iPP and iPP/β-CD-MAH-La were calculated from the full width at half maximum of peak according to the Scherrer equation.[31]

$$D_{hkl} = K\lambda/\beta_0 \cos\theta \quad (3)$$

where D_{hkl} is crystallite size perpendicular to reflection plane (*hkl*) (nm), θ is Bragg angle, λ is wavelength of X-ray used (0.154 nm), β_0 is the full width at half maximum of peak (rad), $K = 0.9$.

Differential scanning calorimetry (DSC)

DSC data of pure iPP and iPP/β-CD-MAH-La was measured with Perkin–Elmer Diamond DSC under nitrogen atmosphere. As for isothermal crystallization, about 10 mg samples were heated quickly from ambient temperature to 220°C and held for 5 min to erase any thermal history. After that, the sample melts were subsequently rapidly cooled at the maximum rate to the predetermined isothermal crystallization temperatures (T_c) and maintained until the crystallization was completed. After crystallization, the samples were reheated to 220°C at the heating rate of 10°C/min.

Polarized light microscopy (PLM)

The spherulitic morphologies of pure iPP and iPP/β-CD-MAH-La were observed with a Leica DMLP polarized optical microscope with hot stage and digital camera. The samples for PLM observation were placed between two glass slides and was heated to 200°C, then squeezed into films and kept at this temperature for 5 min to erase its thermal history. Samples were rapidly cooled to 130°C and maintained until the completion of crystallization to observe the isothermal crystallization process.

RESULTS AND DISCUSSION

Isothermal crystallization structure of iPP with β-CD-MAH-La

WAXD was used to describe the structure and content of β-crystal in iPP during isothermal crystallization. Figure 1 illustrated the WAXD patterns of pure iPP and iPP/β-CD-MAH-La crystallized at 130°C under quiescent condition for 2 h. It was observed that the peaks of 2θ about 14.1°, 16.9°, and 18.5°, corresponding to α(110), α(040), α(130), reflections, were the principal reflections of α-crystal that existed in pure iPP. Whereas, the peak of 2θ about 15.9°, corresponding to β(300) reflection, was the evidence that β-crystal existed in iPP/β-CD-MAH-La. According to eqs. (1) and (2), the value of K_β and X_{all} with different content of β-CD-MAH-La was calculated and listed in Table I. As was seen, X_{all} value was no essential difference for all the samples under identical crystallization condition. However, the K_β value speedily increased with the increase of β-CD-MAH-La, then reached a maximum value (0.84) when the percentage was 0.8 wt %, and finally decreased slightly with further increase of β-CD-MAH-La. Therefore, 0.8 wt % was an optimum addition content for β-CD-MAH-La in the investigating of the

TABLE I
The Value of K_β and X_{all} of iPP with Different Content of β-CD-MAH-La

Sample	X_{all} (%)	K_β (%)
Pure iPP	0.52	0
iPP/0.2 wt % β-CD-MAH-La	0.56	0.32
iPP/0.5 wt % β-CD-MAH-La	0.56	0.53
iPP/0.8 wt % β-CD-MAH-La	0.58	0.84
iPP/1.0 wt % β-CD-MAH-La	0.58	0.76

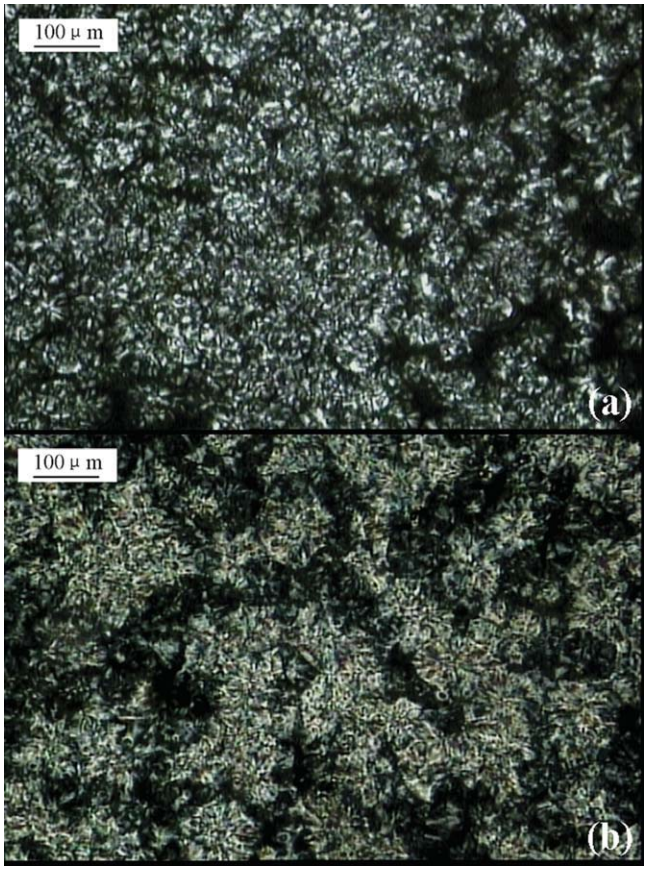

Figure 2 PLM photographs of pure iPP and iPP with 0.8 wt % β-CD-MAH-La crystallized under quiescent conditions. [Color figure can be viewed in the online issue, which is available at wileyonlinelibrary.com.]

isothermal crystallization behavior of β-CD-MAH-La nucleated iPP.

PLM was a visual method for observing the morphology of different crystals and structure. PLM photographs of pure iPP and iPP with 0.8 wt % β-CD-MAH-La crystallized under quiescent conditions was shown in Figure 2. In pure iPP, black and white α spherulites were formed and their boundary was obvious. The α-spherulites were formed mainly by homogeneous nucleation. In iPP/β-CD-MAH-La, a large number of nuclei were induced by β-CD-MAH-La and bright and colored β spherulites emerged. The β-spherulites were formed by heterogeneous nucleation and the spherulites grown fast and overlapped with one another to make the boundary infirmly. Therefore, the spherulite size of iPP/β-CD-MAH-La was much small than that of pure iPP.

The influence of crystallization temperature (T_c) on iPP/β-CD-MAH-La was displayed in Figure 3, which showed that β-crystal formed below 150°C, especially at the range of 110–130°C. Meanwhile, K_β was increased with the increase of isothermal crystallization temperature, then reached a maximum at

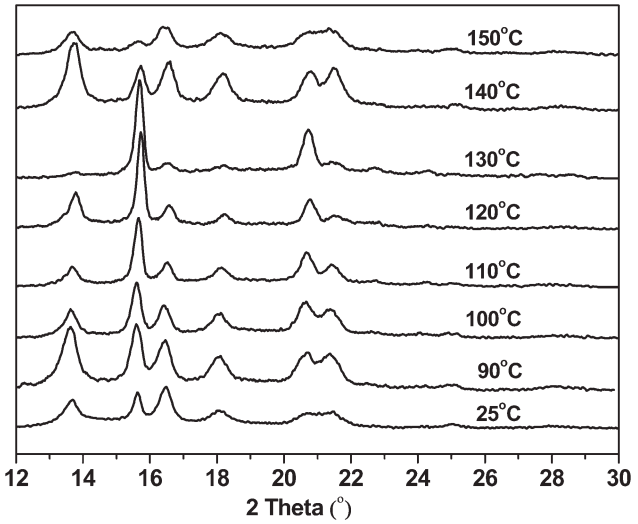

Figure 3 The influence of crystallization temperature (T_c) on iPP/β-CD-MAH-La under quiescent condition for 2 h.

130°C, and finally decreased rapidly. Result verified that the best isothermal crystallization temperature for iPP/β-CD-MAH-La was 130°C, with 150°C probably being the upper temperature. Figure 4 illustrated the evolution of crystal size of perpendicular to the crystal planes β(300) in iPP/β-CD-MAH-La as isothermal crystallization temperature (T_c) rising from 25 to 150°C. $D_{\beta(300)}$ value first increased significantly with increasing T_c, then reached a maximum at 130°C, and finally decreasing rapidly with further increases of T_c. The tendency was similar to that of K_β value.

The isothermal crystallization morphologies of pure iPP and nucleated iPP were observed by PLM and the results were shown in Figure 5. Figure 5(a,b) showed the PLM photographs of pure iPP under isothermal crystallization at 130°C for 30 s

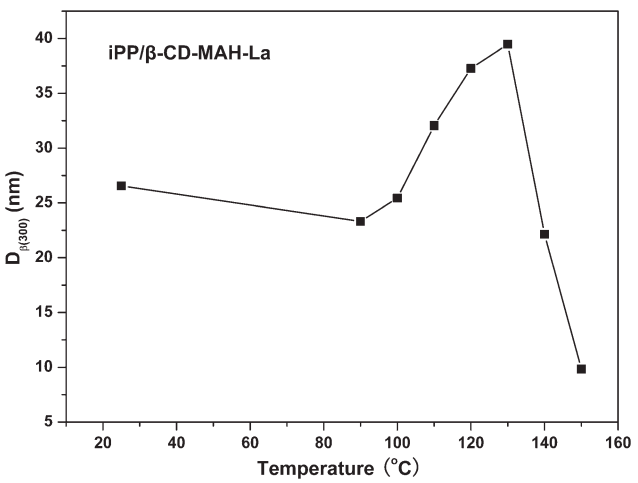

Figure 4 The crystal size perpendicular to the crystal planes β(300) as a function of isothermal crystallization temperature (T_c) of iPP/β-CD-MAH-La.

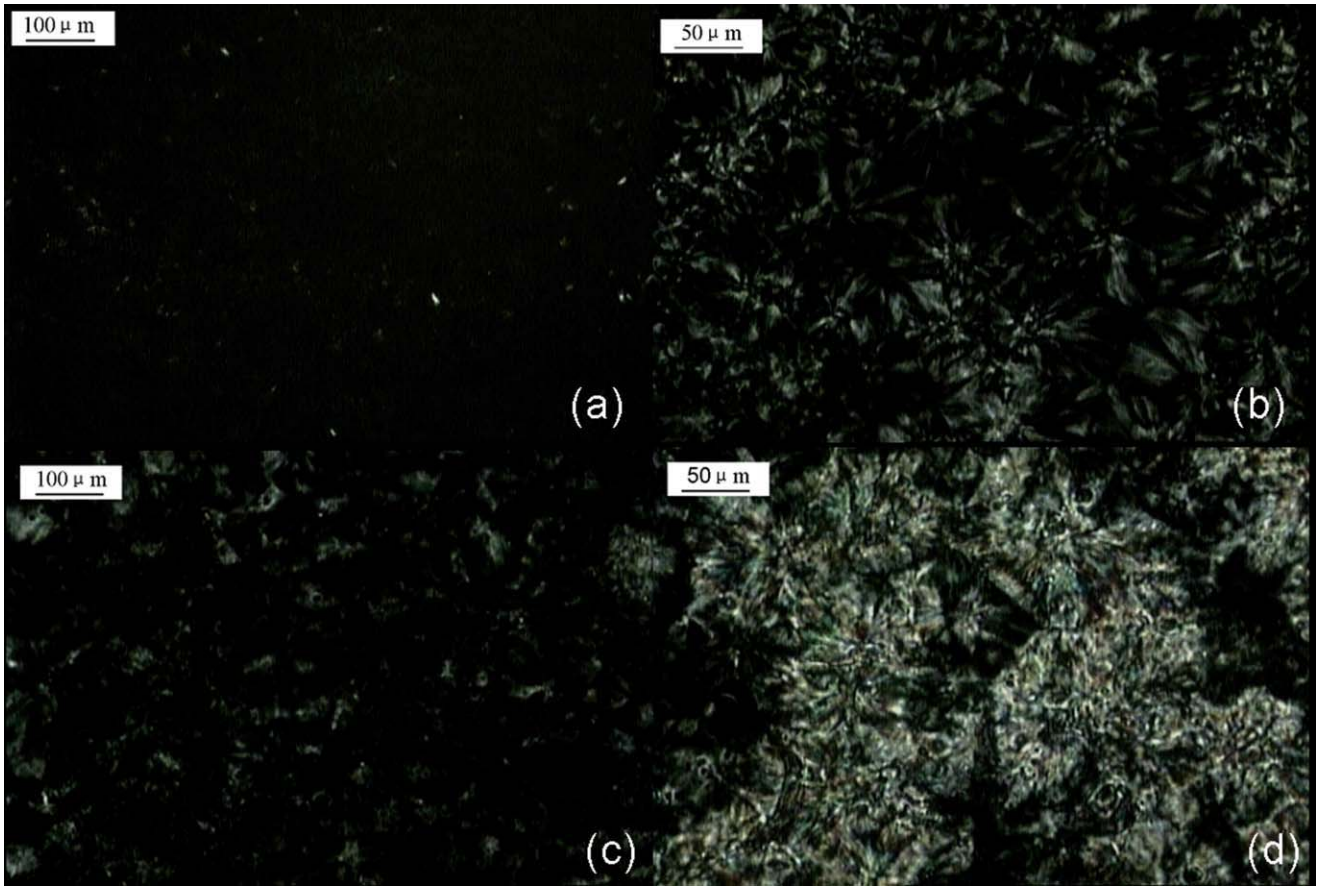

Figure 5 Polarized light microphotographs of pure iPP and iPP/β-CD-MAH-La during isothermal crystallization at 130°C: isothermal crystallization for (a) 30 s and (b) 10 min for pure iPP; and isothermal crystallization for (c) 30 s and (d) 10 min for iPP/β-CD-MAH-La. [Color figure can be viewed in the online issue, which is available at wileyonlinelibrary.com.]

and 10 min, respectively. Figure 5(c,d) showed the PLM photographs of iPP/β-CD-MAH-La for 30 s and 10 min, respectively. It can be observed that the presence of β-CD-MAH-La changed the crystallization process. A number of nuclei appeared in iPP/β-CD-MAH-La while only a few nuclei appeared in pure iPP when the isothermal crystallization time was 30 s. The addition of β-CD-MAH-La could enhance the crystallization rate of iPP due to heterogeneous nucleation effect. Meanwhile, β-CD-MAH-La changed the morphology of iPP. Results demonstrated that β-CD-MAH-La was an effective β-nucleating agent.

Overall kinetics of isothermal crystallization

The crystallization behavior of pure iPP and iPP/β-CD-MAH-La were investigated by DSC. Figure 6 illustrated the crystallization exotherms of iPP and iPP/β-CD-MAH-La during isothermal crystallization. The effect of temperature on crystallization rate of iPP was clearly observed in isothermal thermograms. As crystallization temperature increased, the exothermic peak shifted to longer time and the crystallization time range became broad, which implied that crystallization time became longer and crystallization rate was reduced. From Figure 7, it can be seen that the time required for reaching the exothermic peak, t_p, increased with increasing T_c. Meanwhile, for the same crystallization temperature (125 and 128°C), the presence of β-CD-MAH-La was found to increase the crystallization rate showing especially lower values of t_p for iPP/β-CD-MAH-La compared to pure iPP. Result suggested that β-CD-MAH-La could greatly increase the crystallization rate of iPP due to heterogeneous nucleation.

To obtain more evidence about the isothermal crystallization process, the crystallization kinetics of iPP and iPP/β-CD-MAH-La were compared. The relative crystallinity $X(t)$ can be calculated according to the following equation:

$$X(t) = \frac{\int_0^t (dH/dt)dt}{\int_0^\infty (dH/dt)dt} \quad (4)$$

where dH represents the measured enthalpy of crystallization and dt is the isothermal time interval.

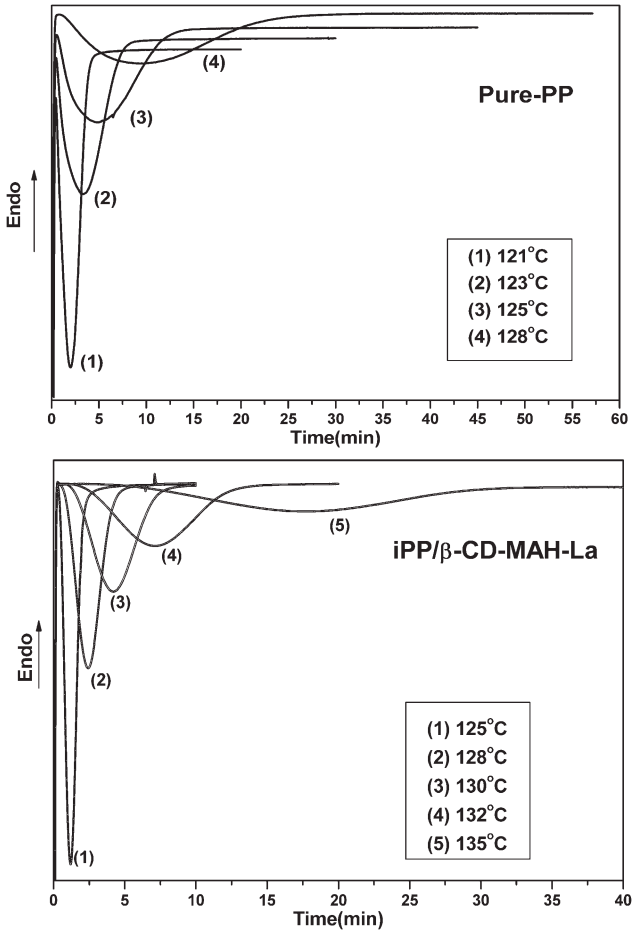

Figure 6 DSC crystallization curves of pure iPP and iPP/β-CD-MAH-La during isothermal crystallization.

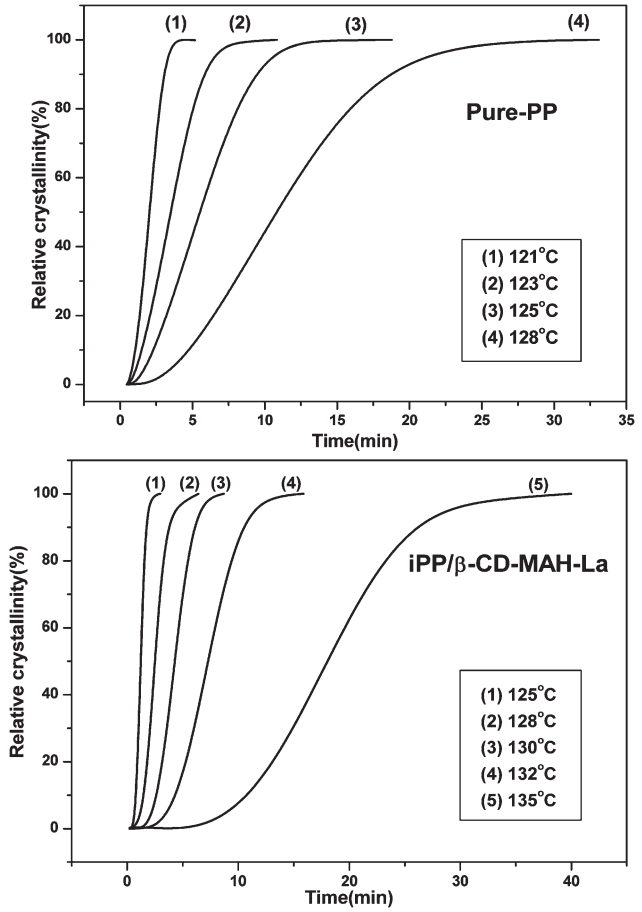

Figure 8 Relative degree of crystallinity as a function of time for pure iPP and iPP/β-CD-MAH-La during isothermal crystallization.

The limits t and ∞ are used to denote the elapsed time during the course of crystallization and at the end of the crystallization process, respectively. The comparison of $X(t)$ as a function of time (t) for iPP and PP/β-CD-MAH-La was shown in Figure 8. It was observed that all these curves showed the same sigmoidal shape, implying only a lag effect of temperature on crystallization.[20] The induction time ($t_{0.05}$), which considered to be the time taken for forming the primary nuclei, is defined as the time for completing 5% conversion[32] and listed in Table II. Meanwhile, the half crystallization time ($t_{0.5}$), that is, the time taken for 50% conversion, is the direct measure of crystallization rate and also listed in Table II. It was apparent that the value of $t_{0.05}$ and $t_{0.5}$ decreased with the increasing of crystallization temperature. Besides, $t_{0.05}$ and $t_{0.5}$ of iPP/β-CD-MAH-La was much small than that of pure iPP at the given crystallization temperature, which proved that β-CD-MAH-La could effectively improve crystallization rate.

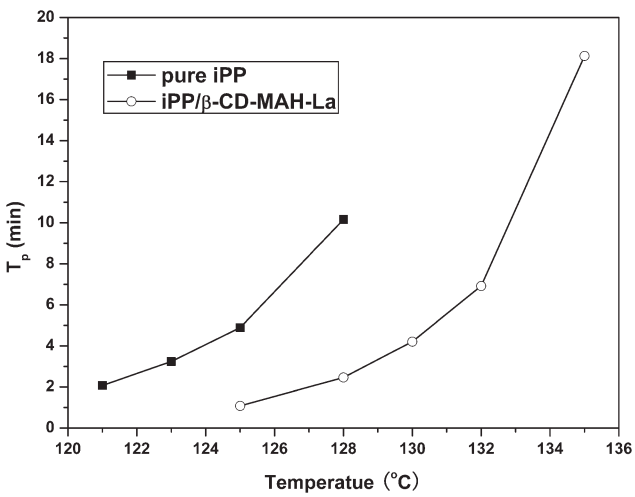

Figure 7 Time at exothermal peak versus T_c for pure iPP and iPP/β-CD-MAH-La.

In addition, the classical Avrami model[27,28] was employed to analyze the isothermal crystallization kinetics of pure iPP and iPP/β-CD-MAH-La, which is the most simple and widely accepted method to analyze the crystallization kinetics of polymers, can be expressed as follows:

$$1 - X(t) = \exp(-kt^n) \quad (5)$$

TABLE II
The Avrami Parameters for Isothermal Crystallization of iPP and iPP/β-CD-MAH-La

Sample	T_c (°C)	$t_{0.05}$ (min)	t_{max} (min)	$t_{0.5}$ (min)	k (min^{-n})	n
Pure iPP	121	0.91	1.90	2.04	8.38×10^{-2}	2.99
	123	1.14	3.25	3.51	3.67×10^{-2}	2.34
	125	1.66	5.03	5.52	1.25×10^{-2}	2.34
	128	3.62	10.02	10.82	1.34×10^{-3}	2.63
					$\overline{n} = 2.59 \pm 0.23$	
iPP/β-CD-MAH-La	125	0.52	1.10	1.14	2.61×10^{-1}	3.89
	128	1.14	2.41	2.40	3.16×10^{-2}	3.30
	130	2.15	4.24	4.15	2.32×10^{-3}	3.86
	132	3.53	7.05	7.29	5.22×10^{-4}	3.58
	135	9.04	18.06	17.95	1.41×10^{-5}	3.68
					$\overline{n} = 3.66 \pm 0.18$	

where t and $X(t)$ are the crystallization time and the relative degree of crystallinity at time t. n is Avrami exponent which depends on the type of nucleation and the growth dimension, and k represents the crystallization rate constant. Equation (5) was liberalized in its logarithmic from to give Eq. (6),

$$\log[-\ln(1 - X(t))] = n \log t + \log k \quad (6)$$

The plots of $\log[-\ln(1 - X(t))]$ as a function of $\log t$ during isothermal crystallization process of iPP and iPP/β-CD-MAH-La were presented in Figure 9. The rate constants (k) and Avrami exponent (n) can be determined directly from the intercept and slope of the best-fitting line. The fitting was performed on the central linear portions of the datasets. The deviation which was observed after linear part in the Avrami equation was probably due to the different growth rate of the two modifications and the onset of secondary crystallization. Also some points in the initial part were not considered because logarithmic plotting tended to overestimate small errors in the assessment of the initial time of crystallization.[31,33] The Avrami parameters, k and n, can be obtained and displayed in Table II. For a particular sample, k decreased with increasing crystallization temperature, which meant that the decreasing of the nucleation rate, and this crystallization behavior was typically observed in a nucleation-controlled temperature region. According to the nucleation and growth mechanism, the Avrami exponent n should be an integer value. However, the value of n reported in the literatures doesn't always match the Avrami equation and shows noninteger, which is caused by some characteristics of polymers, such as secondary crystallization process, mixed nucleation modes, and the change in material density.[34] Besides, some experimental factors, such as an error introduced in the determination of zero point of crystallization and the melting residence time can lead to noninteger values of n.[34,35] In the current work, a value of n of 2.59 ± 0.23 obtained for pure iPP over the crystallization temperature range, was in agreement with Refs. [21] and [34] and the obtained value of n attributed to a homogenous nucleation with two-dimensional growth. However, in the case of iPP/β-CD-MAH-La, the n value was 3.66 ± 0.18, which was due to a change from two-dimensional to three-dimensional crystal growth of the polymer matrix.[34]

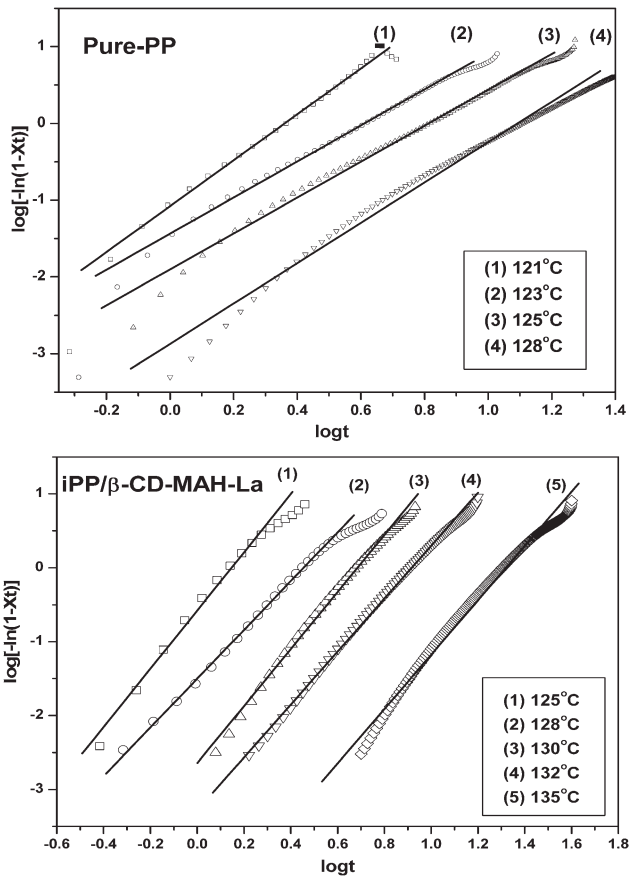

Figure 9 Avrami plots of $\log[-\ln(1 - X(t))]$ *versus* $\log t$ for isothermal crystallization process for pure iPP and iPP/β-CD-MAH-La.

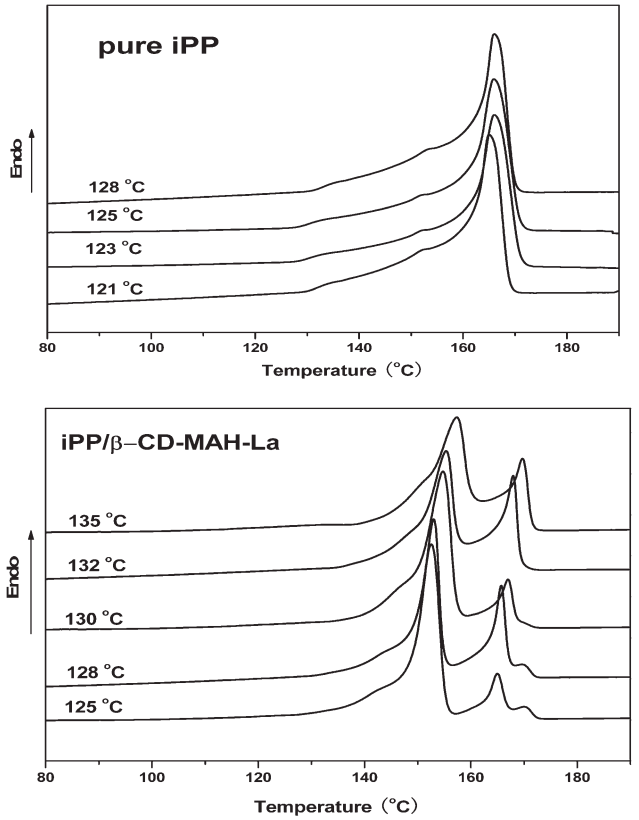

Figure 10 DSC heating curves of pure iPP and iPP/β-CD-MAH-La.

Melting behavior and equilibrium melting points

Melting behavior

After finishing isothermal crystallization, the samples were reheated to 220°C for studying the corresponding melting behavior. As was seen in Figure 10, only one peak at about 166°C was appeared at the observed melting curves of pure iPP, which represented that only α-crystal was presented in pure iPP. While in the curve of iPP/β-CD-MAH-La, there were two peaks at about 167 and 155°C, which were attributed to the melting of the α- and β-crystal, respectively. The phenomenon demonstrated that the β-crystal of iPP can be induced by β-CD-MAH-La. The peaks of α- and β-crystal shifted to higher temperature with increasing crystallization temperature, indicating an increase in the corresponding lamellar thickness.

Equilibrium melting temperature

The equilibrium melting temperature (T_m^0) of a crystalline polymer is defined as the melting temperature of a perfect crystal formed by infinite molecular weight chains,[36] and T_m^0 is an important thermodynamic parameter for understanding the crystallization behavior of polymer systems. In the current work, the equilibrium melting temperature of pure iPP and iPP/β-CD-MAH-La were determined using linear and nonlinear Hoffman-Weeks procedure.[37]

The linear Hoffman-Weeks (LHW) procedure, based on the observed linear relation between melting temperature, T_m, and T_c, is often used to determine $T_{m\mathrm{LHW}}^0$. It is expressed mathematically by the following equation[38]:

$$T_m = \frac{T_c}{\gamma} + \left(1 - \frac{1}{\gamma}\right) T_{m\mathrm{LHW}}^0 \tag{7}$$

The intersection point of the linear extrapolation of T_m versus T_c line with the $T_m = T_c$ line would yield T_m^0. The thickening factor $\gamma = l/l^*$, where l and l^* are the thickness of final lamellar thickness and the initial lamellar thickness, respectively. The linear Hoffman-Weeks (LHW) plots for pure iPP and iPP/β-CD-MAH-La were shown in Figure 11.

However, an important assumption of the linear Hoffman-Weeks is that the thickening factor γ is independent of T_c and t, and the relation between observed T_m and T_c is linear. This assumption has been showed to underestimate the equilibrium melting temperature and overestimate thickening coefficient.[39,40] However, Alamo et al.[41] have explained the nonlinearity in the observed T_m and T_c. Therefore, the equilibrium melting temperature ($T_{m\mathrm{NLHW}}^0$) was calculated by the nonlinear Hoffman-Weeks (NLHW) procedure and used to compare with $T_{m\mathrm{LHW}}^0$.

In this context of the Hoffman-weeks theory,[40] the initial lamellar thickness, l^*, can be expressed in terms of the undercooling ($\Delta T = T_m^0 - T_c$) through the relation:

$$l^* = \frac{2\sigma_e T_m^0}{\Delta H_f(\Delta T)} + C_2 \tag{8}$$

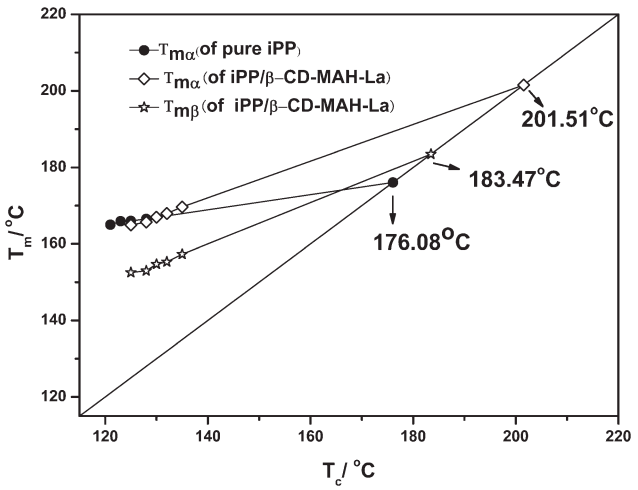

Figure 11 Linear Hoffman-Weeks plot for pure iPP and iPP/β-CD-MAH-La.

TABLE III
Equilibrium Melting Temperature from Nonlinear Hoffman-Week's Extrapolation

Sample	T^0_{mNLHW}	a
α-crystal in pure iPP	198.42	3.42
α-crystal in iPP/β-CD-MAH-La	251.40	2.79
β-crystal in iPP/β-CD-MAH-La	213.69	3.27

where ΔH_f is the heat of fusion per unit volume and σ_e is the fold surface free energy. The term C_2 is a constant, which accounts the term δl and the temperature dependence of the kinetic fold surface free energy, while is always ignored in linear Hoffman-Weeks procedure. Combination of the Gibbs-Thomson equation, $T_m = T^0_m(1 - \frac{2\sigma_e}{l\Delta H_f})$, with $\gamma = \frac{l}{l^*}$ and Eq. (8), leads to the following expression for the observed melting temperature of thickened lamellae formed at T_c.

$$\frac{T^0_m}{T^0_m - T_m} = \gamma \cdot \frac{T^0_m}{\Delta T} + \gamma \cdot \frac{\Delta H_f}{2\sigma_e} \cdot C_2 \tag{9}$$

Marand et al.[39,42] suggested an approach based on the linearization of Eq. (8), which was defined as scaled crystallization and melting temperatures by $X = \frac{T^0_{mNLHW}}{T^0_{mNLHW} - T_c}$ and $M = \frac{T^0_{mNLHW}}{T^0_{mNLHW} - T_m}$, respectively. Therefore, Eq. (9) can be written as:

$$M = \gamma(X + a) \tag{10}$$

where a is equal to $\frac{\Delta H_f C_2}{2\sigma_e}$, and M is only a linear function of X, if γ is constant. Because M and X are defined according to the unknown T^0_{mNLHW}, a range of hypothetical values of T^0_{mNLHW} are substituted in Eq. (10), and calculated a series of corresponding slope, γ, for preparing the plots of γ as a function of T^0_{mNLHW}. And the true T^0_{mNLHW} calculated by the method is found when $\gamma = 1$. The value of T^0_{mNLHW} were listed in Table III.

Comparing with T^0_{mLHW}, the values of T^0_{mNLHW} were higher in all samples, and similar trend have been reported by some studies, where T^0_m was determined by linear and nonlinear Hoffman-Weeks procedure.[37,43,44] The a values for α-crystal in pure iPP determined in the present work was very close to that reported by Xu et al. ($a = 3.45$).[42] T^0_m of both α-crystal and β-crystal in iPP/β-CD-MAH-La became higher with the incorporation of β-CD-MAH-La, which indicated the β-nucleating agent could enhance the crystalline of iPP. The result was in agreement with the characterization by WAXD shown in Table I.

Crystallization activation energy

The process of crystallization involves nucleation and growth. To further investigate the crystal growth kinetics of pure iPP and iPP/β-CD-MAH-La isothermally crystallized from the melt, the secondary nucleation theory proposed by Hoffman-Lauritzen was applied in the current work. According to this theory, the spherulite growth rate (G), defined as $G = \frac{1}{t_{0.5}}$, can be expressed in the form:

$$G = G_0 \exp\left(-\frac{U^*}{R(T_c - T_\infty)}\right) \exp\left(\frac{K_g}{T_c(\Delta T)f}\right) \tag{11}$$

For practical convenient use, Eq. (11) is usually rewritten as follows:

$$\ln G + \frac{U^*}{R(T_c - T_\infty)} = \ln G_0 - \frac{K_g}{T_c(\Delta T)f} \tag{12}$$

where G_0 is a temperature-independent pre-exponential term, U^* is the transport activation energy of polymer segments at the liquid–solid interface, and a universal value of iPP is $U^* = 6280$ J/mol.[34,45] R is the gas constant. $\Delta T = (T^0_m - T_c)$ is the undercooling. T_∞ is the theoretical temperature below which viscous flow ceases, usually defined as $T_\infty = T_g - 30K$). f is a correction factor and defined as $f = \frac{2T_c}{T_c + T^0_m}$. K_g is the nucleation parameter given by the following equation:

$$K_g = \frac{m b_0 \sigma \sigma_e T^0_m}{k_B \Delta H_f} \tag{13}$$

where m is the regime parameter that has a value $m = 4$ for Regime I and III, and $m = 2$ for Regime II.[45] In the current work, the crystallization was assumed to occur in Regime III.[20,42] b_0 is the monolayer thickness. k_B is the Boltzman constant (1.35×10^{-23} J/K), and ΔH_f is the enthalpy of fusion per unit volume. The parameters σ and σ_e are the lateral and fold surface free energies, respectively. Moreover, σ is estimated through using the following equation:

$$\sigma = \alpha(a_0 b_0)^{\frac{1}{2}} \Delta H_f \tag{14}$$

where α is derived empirically to be 0.1 and $a_0 b_0$ is the cross-sectional area of the chain.[45] For iPP, the crystal growth is estimated in favor along α(110) lattice plane of α-crystal during melt-crystallization, and along β(300) lattice plane of β-crystal. The value of ΔH_f and cross-sectional area parameters for α-crystal and β-crystal were listed in Table IV. K_g, calculated from the slop of plot of $\ln G + \frac{U^*}{R(T_c - T_\infty)}$ versus $\frac{1}{T_c(\Delta T)f}$, can be used to obtain the fold surface free energy σ_e. K_g and σ_e of pure iPP and iPP/β-CD-MAH-La were also shown in Table IV.

K_g represents the free energy necessary to form a nucleus of critical size. K_g of α-crystal in iPP/β-CD-MAH-La was higher than that of pure iPP, which

TABLE IV
The Parameters of Lauritzen-Hoffman from Isothermal Crystallization

Sample	ΔH_f (J/m^3)	Growth plane	K_g (K^2) With T^0_{mLHW}	K_g (K^2) With T^0_{mNLHW}	σ_e (mJ/m^2) With T^0_{mLHW}	σ_e (mJ/m^2) With T^0_{mNLHW}
α-crystal in pure iPP	1.96×10^8	(110) $a_0 = 5.49 \times 10^{-10}$ m $b_0 = 6.26 \times 10^{-10}$ m	3.24×10^5 $R^2 = 0.9931$	7.30×10^5 $R^2 = 0.9948$	67.81	145.55
α-crystal in iPP/β-CD-MAH-La			5.46×10^5 $R^2 = 0.9996$	3.02×10^6 $R^2 = 1$	110.58	541.29
β-crystal in iPP/β-CD-MAH-La	1.77×10^8	(300) $a_0 = 6.36 \times 10^{-10}$ m $b_0 = 5.51 \times 10^{-10}$ m	3.37×10^5 $R^2 = 0.9990$	1.08×10^6 $R^2 = 0.9999$	78.81	234.66

indicated that the motion of the α-crystal chains was more difficult in iPP/β-CD-MAH-La. However, in iPP/β-CD-MAH-La, K_g of β-crystal was much lower than that of α-crystal. It proved that β-CD-MAH-La can act as effective β-nucleating agents for iPP. The decrease of σ_e could indicate an increase in the entropy of folding and therefore the formation of less homogeneous and regular folding surface.[46] The addition of β-CD-MAH-La reduced the creation of new surface for β-crystal, hence leading to faster crystallization rate. Moreover, the K_g values were sensitive to T^0_m, and higher T^0_m values were obtained if $T^0_m = T^0_{mNLHW}$ was used.

CONCLUSIONS

The effects of β-CD-MAH-La as β-nucleating agent on the crystal structure and the isothermal crystallization behavior of iPP were studied in the current work. WAXD results indicated that the addition of β-CD-MAH-La effectively induced the form of β-crystal in iPP. Under isothermal conditions, the content of β-crystal of iPP/β-CD-MAH-La was influenced by β-CD-MAH-La content and isothermal crystallization temperature. Moreover, β-CD-MAH-La nucleating agent has succeeded in promoting greater rate of crystallization in iPP. The melting temperature of α- and β-crystal was increased with the increasing T_c. The equilibrium melting temperature determined by nonlinear Hoffman-Weeks procedure was higher than that of linear Hoffman-Weeks procedure. The equilibrium melting temperature of both α-crystal and β-crystal in iPP/β-CD-MAH-La became higher with the incorporation of β-CD-MAH-La, which indicated that the β-nucleating agent could enhance the crystalline of iPP. In addition, it revealed that the motion of the α-crystal chains was more difficult in iPP/β-CD-MAH-La as compared with pure iPP, by the analysis of the nucleation parameter (K_g) and activation energy (σ_e) of crystallization Regime III of iPP/β-CD-MAH-La. The addition of β-CD-MAH-La reduced the creation of new surface for β-crystal, therefore it led to faster crystallization rate.

References

1. Varga, J. J Macromol Sci B 2002, 41, 1121.
2. Xiao, W.; Wu, P.; Feng, J. J Appl Polym Sci 2008, 108, 3370.
3. Mohmeyer, N.; Schmidt, H. W.; Kristiansen, P. M.; Altstadt, V.; Macromolecules 2006, 39, 5760.
4. Chen, H. B.; Karger-Kocsis, J.; Wu, J. S.; Varga, J. Polymer 2002, 43, 6505.
5. Shi, G.; Zhang, X. Thermochim Acta 1992, 205, 235.
6. Mathieu, C.; Thierry, A.; Wittmann, J. C.; Lotz, B. J Polym Sci Part B Polym Phys 2002, 40, 2504.
7. Liu, M. X.; Guo, B. C.; Du, M. L.; Chen, F.; Jia, D. M. Polymer 2009, 50, 3022.
8. Leugering, H. J. J Macromol Chem 1967, 109, 204.
9. Garbarczyk, J.; Paukszta, D. Colloid Polym Sci 1985, 263, 985.
10. Ikeda, N.; Kobayashi, T.; Killough, L. In Polypropylene '96. World Congress, Zurich, Switzerland, 1996.
11. Varga, J.; Menyhard, A.; Macromolecules 2007, 40, 2422.
12. Shi, G. Y.; Zhang, X. D.; Qiu, Z. X. Macromol Chem Phys 1992, 193, 583.
13. Shi, G.; Huang, B.; Zhang, J. Makromol Chem Rapid Commun 1984, 5, 573.
14. Varga, J.; Mudra, I.; Ehrenstein, G. W. J Appl Polym Sci 1999, 74, 2357.
15. Zhang, Z.; Wang, C.; Yang, Z.; Chen, C.; Mai, K. Polymer 2008, 49, 5137.
16. Su, Z. Q.; Dong, M.; Guo, Z. X.; Yu, J. Macromolecules 2007, 40, 4217.
17. Phillips, A.; Zhu, P. W.; Edward, G. Polymer 2010, 51, 1599.
18. Yang, J.; Pan, P.; Dong, T.; Inoue, Y. Polymer 2010, 51, 807.
19. Supaphol, P. Thermochim Acta 2001, 370, 37.
20. Lonkar, S. P.; Singh, R. P. Thermochim Acta 2009, 491, 63.
21. Marco, C.; Ellis, G.; Gomez, M. A.; Arribas, J. M. J Appl Polym Sci 2003, 88, 2261.
22. Huo, H.; Jiang, S. C.; An, L. J.; Feng, J. C. Macromolecules 2004, 37, 2478.
23. Shentu, B.; Li, J.; Gan, T.; Weng, Z. Eur Polym Mater 2007, 43, 3036.
24. Bai, H.; Wang, Y.; Zhang, Q.; Liu, L.; Zhou, Z. J Appl Polym Sci 2009, 111, 1624.
25. Zhao, S.; Cai, Z.; Xin, Z. Polymer 2008, 49, 2745.
26. Zhang, Z.; Chen, C.; Wang, C.; Guo, J.; Mai, K. J Therm Anal Calorim 2010, 103, 311.
27. Avrami, M. J. J Chem Phys 1939, 7, 1103.
28. Avrami, M. J. J Chem Phys 1940, 8, 212.
29. Hoffman, J. D.; Davis, G. T.; Lauritzen, J. I. In Treatise on Solid State Chemistry; Plenum Press: New York, 1976.
30. Turner-Jones, A.; Aizlewood, J. M.; Beckett, D. R. Macromol Chem 1964, 75, 134.
31. Raka, L.; Sorrention, A.; Bogoeva-Gaceva, G. J Polym Sci Part B Polym Phys 2010, 48, 1927.
32. Balamurugan, G. P.; Maiti, S. N. J Appl Polym Sci 2008, 107, 2414.

33. Papageorgiou, G. Z.; Achilias, D. S.; Bikiaris, D. N.; Karayannidis, G. P. Thermochim Acta 2005, 427, 117.
34. Naffakh, M.; Martin, Z.; Marco, C.; Gomez, M. A.; Jimenez, I. Thermochim Acta 2008, 472, 11.
35. Yu, J.; He, J. Polymer 2000, 41, 891.
36. Wu, P. L.; Woo, E. M. J Polym Sci Part B Polym Phys 2002, 40, 1571.
37. Juhasz, P.; Varga, J.; Belina, K.; Marand, H. J Therm Anal Calorim 2002, 69, 561.
38. Hoffman, J. D.; Weeks, J. J. J Res Natl Bur Stand Sect A 1962, 66A, 13.
39. Marand, H.; Xu, J.; Srinivas, S. Macromolecules 1998, 31, 8219.
40. Hoffman, J. D.; Miller, R. L. Polymer 1997, 38, 3151.
41. Alamo, R. G.; Viers, B. D.; Mandelkern, L. Macromolecules 1995, 28, 3205.
42. Xu, J.; Srinivas, S.; Marand, H. Macromolecules 1998, 31, 8230.
43. Huang, J. Polym Eng Sci 2009, 49, 1855.
44. Deshpande, V. D.; Jade, S. J Appl Polym Sci 2010, 116, 3541.
45. Clark., E. J.; Hoffman, J. D. Macromolecules 1984, 17, 878.
46. Beck, H. N. J Appl Polym Sci 1975, 19, 371.